Biophysical Chemistry 27 (1987) 233–241
Elsevier

BPC 01173

Demonstration of an associated anisotropy decay by frequency-domain fluorometry

Henryk Szmacinski, Ranjith Jayaweera, Henryk Cherek and Joseph R. Lakowicz

University of Maryland at Baltimore, School of Medicine, Department of Biological Chemistry, 660 West Redwood Street, Baltimore, MD 21201, U.S.A.

Received 30 March 1987
Accepted 7 May 1987

Frequency-domain fluorometry; Fluorescence anisotropy; Anisotropy decay; Rotational diffusion

We used frequency-domain fluorometry to demonstrate the presence of an associated decay of fluorescence anisotropy. In such systems the individual correlation times are associated with distinct emitting species, each with its own characteristic lifetime and rotational correlation times. We obtained an associated system using 1-anilino-8-naphthalenesulfonic acid (ANS) in the presence of increasing amounts of apomyoglobin. When both free and apomyoglobin-bound ANS contributed to the emission the differential polarized phase angles become negative at particular frequencies, even though the fundamental anisotropy (r_0) is greater than zero. Additionally, the modulated anisotropy decreases at high frequencies. Both observations appear to be the unique consequence of an associated anisotropy decay, and are not possible for a multiexponential anisotropy decay of a single species.

1. Introduction

Time-dependent decays of fluorescence anisotropy are often used to estimate the size, shape and flexibility of biological macromolecules [1–5]. The anisotropy decays are usually multiexponential and reveal time-dependent rotational displacements of the fluorescent residue. These displacements are due to both rotational diffusion of the entire macromolecule and local motions of the emitting species. Frequently, time-resolved intensity decays are also more complex than a single exponential. The heterogeneity can be intrinsic to a single type of emitting species, and may have a variety of origins including populations of conformers [6,7], excited-state processes [8,9] or transient effects in quenching [10,11]. We refer to such systems as nonassociative, in that the individual decay times are not associated with individual correlation times in the anisotropy decay [12]. Alternatively, the intensity and anisotropy decays can be multiexponential due to the presence of multiple emitting species, each of which displays a discrete intensity decay and a discrete anisotropy decay. For instance, the emission from a mixture of two single-tryptophan proteins may be considered to be an associated system. The tryptophan intensity decay of each protein is associated with the anisotropy decay of each protein.

Associated and nonassociated systems have been studied in the time domain [12–14]. In these studies it was possible to recover the emission spectra of the individual species based on their distinct correlation times. In this report we describe the alternative frequency-domain measurements for an associated system. As a model, we chose 1-anilino-8-naphthalenesulfonic acid (ANS) which binds to the heme pocket of apomyoglobin

Correspondence address: J.R. Lakowicz, University of Maryland at Baltimore, School of Medicine, Department of Biological Chemistry, 660 West Redwood Street, Baltimore, MD 21201, U.S.A.

with an approx. 400-fold increase in intensity [15]. By use of limited amounts of apomyoglobin it was possible to obtain significant emission from both free and bound ANS. The frequency-domain data for this system displayed unique features, which we believe are only possible for an associated system. These features are negative differential phase angles when $r_0 > 0$, and modulated anisotropies which decrease at high modulation frequencies. While a failure to observe these features does not prove a system to be nonassociative, observation of these features demonstrates that the emission is due to more than a single species. Realization of these features of an associated system may be valuable in interpreting the frequency-domain anisotropy data from other complex systems.

2. Theory

2.1. Associated and nonassociated anisotropy decays

The unique features of an associated anisotropy decay are best described in comparison with a nonassociated decay. For simplicity, we will only consider models in which there are two decay times and two correlation times. For the nonassociated case the two decay times and two correlation times are characteristic of the heterogeneous intensity decay of the fluorophore and rotational motions which are too complex to be described by a single correlation time. That is, the sample contains one emitting species, whose intensity and anisotropy decays are both double exponentials. For an associated decay we assume the sample contains two emitting species, each of which displays a single decay time and a single correlation time. This is clearly an approximation, in that each species can itself be more complex than a single exponential. However, this simple model illustrates the unique features of an associated decay, and it is adequate for the ANS-apomyoglobin system described in this report.

Anisotropy decays are determined from measurements of the time-dependent decays of the polarized components of the emission. Following δ-function excitation, the parallel ($\|$) and perpendicular ($\perp$) components of the intensity decay are [5]

$$I_{\|}(t) = \tfrac{1}{3} I_0(t)[1 + 2r(t)] \tag{1}$$

$$I_{\perp}(t) = \tfrac{1}{3} I_0(t)[1 - r(t)]. \tag{2}$$

In these expressions $I_0(t) = I_{\|}(t) + 2I_{\perp}(t)$ is the rotation-free intensity decay and $r(t)$ the anisotropy decay. Both decays ($I_0(t)$ and $r(t)$) are usually described as the sum of exponentials. For our specific case of a double exponential we have

$$I_0(t) = \alpha_1 e^{-t/\tau_1} + \alpha_2 e^{-t/\tau_2} \tag{3}$$

$$r(t) = \beta_1 e^{-t/\theta_1} + \beta_2 e^{-t/\theta_2} \tag{4}$$

The meaning of the intensity decay parameters (α_i and τ_i) depends upon whether the system is associated or nonassociated. For the nonassociated case the values of α_i and τ_i are characteristic of the single species in the sample. The multiexponential intensity decay can have a variety of origins [6–11], but it is generally difficult to prove the molecular origin of the complexity. The meaning of α_i and τ_i is simple for the associated case. The values of τ_1 and τ_2 are the decay times of the two emitting species. The fraction of the total emission from each species is given by

$$f_i = \frac{\alpha_i \tau_i}{\sum \alpha_i \tau_i} \tag{5}$$

In a similar manner the parameters describing the anisotropy decay (β_j and θ_j) have a different meaning for the nonassociated and the associated cases. For a single emitting species (nonassociated) the anisotropy decay is characteristic of this species, and reflects the size, shape and flexibility of the rotating unit. For instance, if the species is asymmetric and displays two correlation times then

$$r(t) = r_0 g_1 e^{-t/\theta_1} + r_0 g_2 e^{-t/\theta_2} \tag{6}$$

where the correlation times and their amplitudes ($r_0 g_j$, $\Sigma g_j = 1.0$) are determined by the rates of rotation about the principal axes and by the orientation of the excitation and emission moments with these axes, respectively [3]. The value of r_0 is characteristic of the fluorophore in the absence of rotational diffusion.

The meaning of the anisotropy decay parame-

ters is different when there are two emitting species. It is known [1,16] that the observed anisotropy from a mixture is the intensity-weighted average of the anisotropies of the two species. This is true at all times, so

$$r(t) = r_1(t)f_1(t) + r_2(t)f_2(t) \tag{7}$$

where $r_i(t)$ are the individual anisotropy decays and $f_i(t)$ the time-dependent fractional intensities,

$$f_i(t) = \frac{\alpha_i e^{-t/\tau_i}}{\alpha_1 e^{-t/\tau_1} + \alpha_2 e^{-t/\tau_2}} \tag{8}$$

Eqs. 7 and 8 allow for a variety of anisotropy decays, many of which are not distinguishable from the associated decays [17]. It is not our intention to describe all possible cases, but we wish to point out that the associated case can predict time-dependent anisotropies which increase at longer times, which is not possible for the nonassociated case with $r_0 > 0$. For instance, consider a system in which the fluorophore exists in two states, both free in solution and bound to a protein, with correlation times of 0.2 and 10 ns, respectively. Assume further that the decay time of the fluorophore increases substantially upon binding to the protein, from 0.5 ns in solution to 10 ns in the bound form. Then, at early times (< 0.5 ns) the fractional intensity of the free form is dominant, and the anisotropy decays rapidly because of the short correlation time of the free fluorophore (fig. 1, unbroken line). At longer times the emission from the bound form dominates, and the anisotropy increases, becoming comparable to that of the bound fluorophore. In contrast, these same parameters result in a monotonically decreasing anisotropy if the decay is nonassociative (fig. 1, broken line: eq. 6).

2.2. *Frequency-domain anisotropy decays*

In the frequency domain the measured quantities are the phase angle shift between the parallel and perpendicular components of the emission ($\Delta\omega$) and the ratio of the amplitudes of the parallel ($m_\parallel$) and perpendicular ($m_\perp$) components of the modulated emission ($\Lambda_\omega = m_\parallel / m_\perp$), measured over a range of modulation frequencies (ω) [18,19].

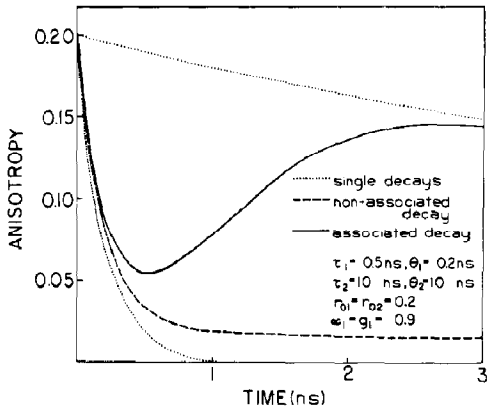

Fig. 1. Simulated time-domain anisotropy decays for associated and nonassociated systems. The assumed decay times are $\tau_1 = 0.5$ and $\tau_2 = 10$ ns, the assumed correlation times being $\theta_1 = 0.2$ and $\theta_2 = 10$ ns. The dotted lines show the anisotropy decays for single correlation times of 0.2 and 10 ns. Also shown are the simulated data for an associated decay with $r_{01} = r_{02} = 0.2$ and $\alpha_1 = 0.90$ (———), and for a nonassociated decay with $g_i = 0.90$ (- - - - - -) and $\Sigma r_0 g_i = 0.2$.

For any values of the parameters or form of the decays these values can be calculated (c) from the sine and cosine transformations of the polarized components of the decays,

$$\Delta_{c\omega} = \arctan\left[\frac{D_\parallel N_\perp - N_\parallel D_\perp}{N_\parallel N_\perp + D_\parallel D_\perp}\right] \tag{9}$$

$$\Lambda_{c\omega} = \left[\frac{N_\parallel^2 + D_\parallel^2}{N_\perp^2 + D_\perp^2}\right]^{1/2} \tag{10}$$

where

$$N_k = \int_0^\infty I_k(t) \sin \omega t \, dt \tag{11}$$

$$D_k = \int_0^\infty I_k(t) \cos \omega t \, dt \tag{12}$$

and k indicates the polarization ($\parallel$ or $\perp$).

The transforms (N_k and D_k) take on different forms depending upon whether the decay is associated or nonassociated. For the nonassociated

case these transforms are

$$N_{\parallel} = \frac{1}{3}\sum_{i=1}^{2}\frac{\alpha_i\omega}{\omega^2+\Gamma_i^2} + \frac{2}{3}\sum_{j=1}^{2}\frac{\alpha_1\omega r_0 g_j}{\omega^2+(\Gamma_1+6R_j)^2} + \frac{2}{3}\sum_{j=1}^{2}\frac{\alpha_2\omega r_0 g_j}{\omega^2+(\Gamma_2+6R_j)^2} \quad (13)$$

$$D_{\parallel} = \frac{1}{3}\sum_{i=1}^{2}\frac{\alpha_i\Gamma_i}{\omega^2+\Gamma_i^2} + \frac{2}{3}\sum_{j=1}^{2}\frac{\alpha_1(\Gamma_1+6R_j)r_0 g_j}{\omega^2+(\Gamma_1+6R_j)^2} + \frac{2}{3}\sum_{i=1}^{2}\frac{\alpha_2(\Gamma_2+6R_j)r_0 g_j}{\omega^2(\Gamma_2+6R_j)^2} \quad (14)$$

where $\Gamma_i = 1/\tau_i$ and $6R_j = 1/\theta_j$. The expressions for the perpendicular components are similar except that the factor of $2/3$ is replaced by $-1/3$. It is instructive to state explicitly which terms in eqs. 13 and 14 are known and which are determined from the anisotropy data. At present, we perform a separate measurement to determine the rotation-free intensity decay. Hence, the values of α_i and $\Gamma_i = 1/\tau_i$ are known. The least-squares analysis determines the values of $\theta_j = (6R_j)^{-1}$ and $r_0 g_j$ which are most consistent with the data. The values of θ_j and $r_0 g_j$ are characteristic of a single species with more than one correlation time.

The expressions for N_k and D_k are different for an associated decay. Substitution of eq. 7 into eqs. 11 and 12 yields

$$N_{\parallel} = \frac{1}{3}\sum_{i=1}^{2}\frac{\alpha_i\omega}{\omega^2+\Gamma_i^2} + \frac{2}{3}\left[\frac{\alpha_1 r_{01}\omega}{\omega^2+(\Gamma_1+6R_1)^2} + \frac{\alpha_2 r_{02}\omega}{\omega^2+(\Gamma_2+6R_2)^2}\right] \quad (15)$$

$$D_{\parallel} = \frac{1}{3}\sum_{i=1}^{2}\frac{\alpha_i\Gamma_i}{\omega^2+\Gamma_i^2} + \frac{2}{3}\left[\frac{\alpha_1 r_{01}(\Gamma_1+6R_1)}{\omega^2+(\Gamma_1+6R_1)^2} + \frac{\alpha_2 r_{02}(\Gamma_2+6R_2)}{\omega^2+(\Gamma_2+6R_2)^2}\right] \quad (16)$$

where r_{0j} is the fundamental anisotropy ($t = 0$) of each species. If the intensity decay (α_i and τ_i) is known then the unknown terms are the correlation times ($\theta_j = 1/6R_j$) and the fundamental anisotropies (r_{0j}) of each species. Alternatively, it is possible to use the known values of r_{0j}, which can usually be determined by a separate experiment. In this case the analysis yields the correlation times and preexponential factors (α_i), which in turn were used to calculate the fractional intensities due to each species (eq. 5).

Under appropriate circumstances the frequency-domain data for an associated anisotropy decay can display unique and unexpected features. If the decay is nonassociated, and $r_0 > 0$, then each correlation time yields a Lorentzian distribution of the differential phase angles when plotted vs. log-frequency. (More precisely, the tangent of Δ_ω vs. log-frequency is a Lorentzian.) Additionally, the modulated anisotropies increase monotonically with frequency, and at high frequencies approach r_0, which is 0.2 for these simulations. For a 10 ns correlation time the differential phase angle is maximal near 30 MHz (fig. 2). For the 0.2 ns correlation time the maximum of the differential phase angles is displayed beyond the 200 MHz limit used for these stimulations. Nonetheless, it is possible to recover such values from 200 MHz data.

Surprisingly different data are expected for an

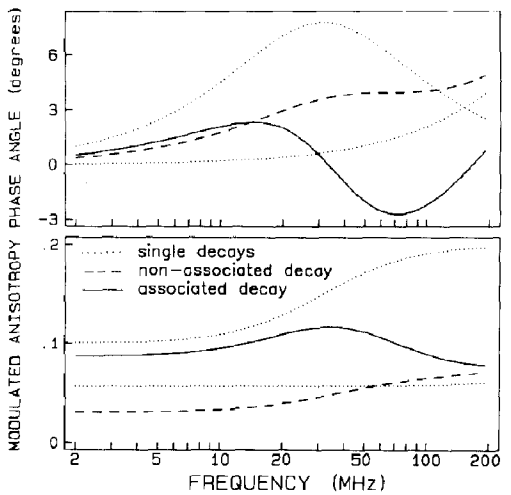

Fig. 2. Simulated frequency-domain anisotropy data for associated and nonassociated decays. Parameters are the same as in fig. 1.

associated decay. In this case, the differential phase angles increase with frequency, then decrease to negative values, followed by an increase at still higher frequencies. Additionally, the modulated anisotropies decrease at the higher frequencies, rather than increasing towards r_0 as occurs for the nonassociated case. To the best of our knowledge, negative phase angles with $r_0 > 0$ and decreasing modulated anisotropies are unique features of an associated anisotropy decay.

3. Materials and methods

Apomyoglobin was a gift from Professor E. Bucci, and was prepared from sperm-whale myoglobin as described previously [20,21]. All measurements were performed at 4°C in 0.1 M phosphate (pH 7.0). The concentration of apomyoglobin was calculated from the absorption at 280 nm using $\epsilon = 14455\ M^{-1}\ cm^{-1}$. The concentrations of ANS were calculated from the absorbance at 350 nm using $\epsilon = 5000\ M^{-1}\ cm^{-1}$.

Frequency-domain data were obtained as described previously [22]. The excitation source was an HeCd laser at 325 nm. This source was modulated at the desired frequency using a Lasermetrics 1042 electro-optic modulator. The emission was observed through a Corning 0-52 filter. For measurement of the intensity decays the excitation was polarized vertically, and the emission at 54.7° from the vertical, to provide a rotation-free result. At −60°C in propylene glycol we found $r_0 = 0.189$ for ANS excited at 325 nm.

The data were analyzed by the method of nonlinear least squares [18,19,23] minimizing the value of χ^2_R. The uncertainties in the phase and modulation values were taken as 0.2° and 0.005, respectively, for both the intensity and anisotropy decay analysis.

4. Results

Emission spectra of ANS with increasing amounts of apomyoglobin are shown in fig. 3. In the absence of apomyoglobin the emission is weak and the maximum is near 513 nm. The addition of

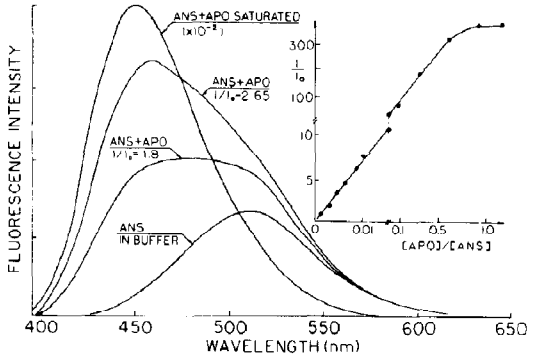

Fig. 3. Emission spectra of ANS with increasing amounts of apomyoglobin. The inset shows the relative increase in integrated intensity, over ANS alone.

low molar ratios of apomyoglobin (less than 0.01) results in an increase in ANS intensity and a shift of the emission towards shorter wavelengths. When the apomyoglobin/ANS ratio reaches unity the intensity of ANS increases 350-fold, and the emission maximum is at 450 nm. This shift is attributed to the binding of ANS to the hydrophobic heme pocket [15]. When the amount of apomyoglobin is not adequate for complete binding of the ANS the emission spectrum is more widely distributed on the wavelength scale, which is obviously due to emission from both the free and bound forms of ANS. To observe significant emission from both forms of ANS it is necessary to use low molar ratios of apomyoglobin to ANS. Otherwise, the more highly fluorescent complex dominates the emission.

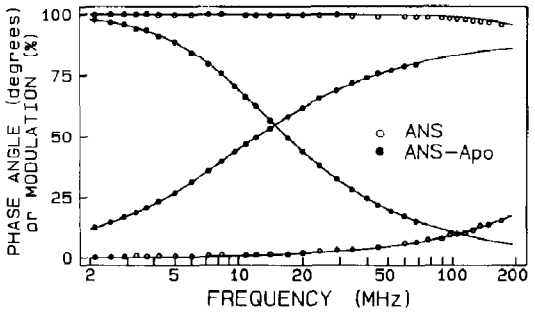

Fig. 4. Frequency response of the intensity decay of ANS alone (○) and of ANS completely bound to apomyoglobin (●). The solid lines are the best single decay time fit for ANS alone, and the best two decay time fit for ANS-apomyoglobin (table 1).

Binding of ANS to apomyoglobin results in a substantial increase in its lifetime. This is seen from fig. 4, which shows the frequency response for the total emission of ANS (○) and for the apomyoglobin-ANS complex (●). Upon binding to apomyoglobin the ANS frequency response shifts dramatically towards lower frequencies, which is indicative of a longer lifetime. In water the lifetime of ANS is 0.26 ns, which increases to 15.8 ns when bound to apomyoglobin. It is possible to recover two decay times for the complex, but the use of two decay times unnecessarily complicates the anisotropy analysis.

The frequency response of ANS becomes extremely heterogeneous when significant emission occurs from the free and bound forms (fig. 5). One notices that the modulation does not approach zero and that the phase angle decreases at high frequencies. The extreme heterogeneity is also apparent from attempts to fit the data to a single decay time (table 1). The values of χ^2_R increase towards 9000 for an apomyoglobin/ANS ratio of 0.01, and then decrease to 18.6 as the emission becomes dominated by the ANS-apomyoglobin complex. At each apomyoglobin/ANS ratio we recovered essentially the same two decay times,

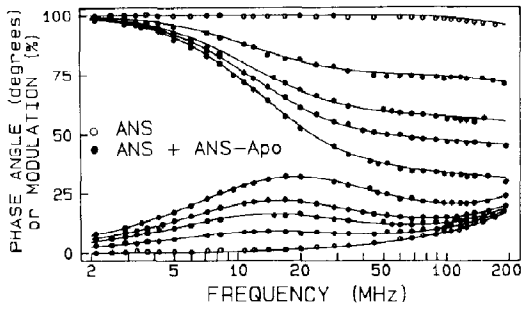

Fig. 5. Frequency-domain intensity decay of ANS alone (○) with increasing amounts of apomyoglobin (●). The curves with increasing phase angles and decreasing modulation represent increasing apomyoglobin/ANS molar ratios of 0.0012, 0.0032, 0.0047 and 0.0087. The intensity decay data for the ratio 0.0047 are not given in tables 1 or 2.

which we attribute to the free and bound forms of ANS. The multiexponential lifetime analysis reveals the fractional emission from each form. As the apomyoglobin/ANS ratio is increased from 0 to 1 the fraction of the emission from the bound form also increases from 0 to 1.

Frequency-domain anisotropy data for ANS in solution (○) and bound to apomyoglobin (●) are

Table 1

Intensity decays of ANS with variable binding to apomyoglobin (Apo)

[Apo]/[ANS]	$\exp(-t/\tau)$		$\sum_{i=1}^{2} \exp(-t/\tau_i)$			
	τ (ns)	χ^2_R	τ (ns)	α_i	f_i	χ^2_R
0	0.26	1.8	0.26	0.9997	0.991	0.9
			9.00	0.0003	0.009	
0.0012	0.368	948.0	0.25	0.994	0.743	3.0
			14.98	0.006	0.257	
0.0032	0.51	2 667.0	0.25	0.988	0.569	3.0
			15.79	0.012	0.431	
0.0087	1.07	7 308.0	0.27	0.964	0.316	2.2
			15.81	0.036	0.684	
0.0158	3.02	8 641.0	0.26	0.929	0.176	1.3
			15.83	0.071	0.824	
0.0474	9.43	3 613.0	0.30	0.834	0.090	2.5
			15.36	0.167	0.910	
0.0790	11.32	2 365.0	0.27	0.755	0.052	1.6
			15.15	0.245	0.948	
1.183	15.67	18.6	4.76	0.130	0.040	0.6
			16.78	0.871	0.960	

shown in fig. 6. In the bound form the differential phase angles are distributed nearly as a Lorentzian with a maximum near 20 MHz. The modulated anisotropy increases monotonically with frequency, and the high-frequency limit of 0.19 is close to the expected value of ANS when excited at 325 nm, which is 0.189. The single correlation time analysis yields a value of 13.2 ns (table 2). The data for free ANS are somewhat different due to its shorter correlation time. The small increase in Δ_ω above 100 MHz and the relatively constant value of Λ_ω are consistent with a correlation time near 100 ps. It is possible to obtain a more highly resolved anisotropy decay for ANS using data measured at higher modulation frequencies [24], but this is not needed for the present analysis.

The frequency response for the polarized emission is remarkably different when both forms of ANS contribute to the emission (fig. 7). Then, the differential phase angles become negative around 20–100 MHz. Additionally, the modulated anisotropies reach a maximum and then decrease at higher frequencies. To the best of our knowledge these are unique features of an associated anisotropy decay. The data can be analyzed to recover the individual correlation times and the apparent values of r_0 for each species (table 2). As expected,

Table 2

Anisotropy decays of ANS with variable binding to apomyoglobin (Apo)

[Apo]/[ANS]	θ_1 (ps)	θ_2 (ns)	r_{01}	r_{02}	χ^2_R
0	97	–	0.222	–	1.40
0.0012	147	11.71	0.184	0.181	1.27
0.0032	154	13.42	0.172	0.170	0.92
0.0087	182	14.12	0.160	0.170	1.23
0.0158	166	14.62	0.242	0.170	1.0
0.0474	194	15.07	0.293	0.177	1.4
0.079	251	14.49	0.248	0.178	1.0
1.183	–	13.24	–	0.188	1.1
0–1.183 (global)	138	12.14	0.188	0.189	8.51

essentially the same value of the correlation times and r_{0j} values were recovered for a range of apomyoglobin/ANS ratios. As the emission from ANS becomes smaller the recovered values of r_0 become more variable (table 2). This is particularly noticeable for a molar ratio of 0.0474, where the free ANS contributes only 10% to the total emission (table 1). The data were also analyzed globally to recover just four parameters (θ_1, θ_2, r_{01} and r_{02}) from the data at nine apomyoglobin/ANS ratios. The parameter values are acceptable, but the value of χ^2_R is elevated from about 1.2 for the

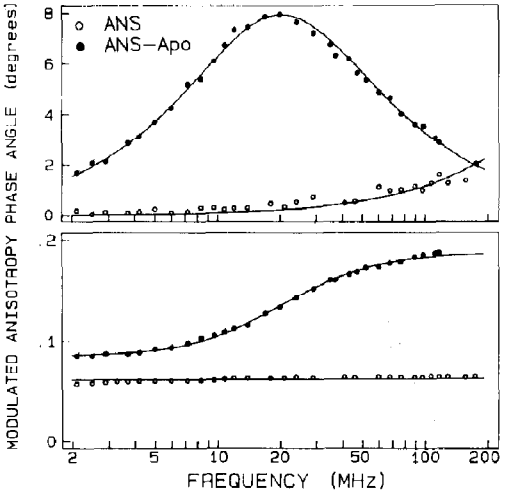

Fig. 6. Frequency-domain anisotropy decays of apomyoglobin-ANS (●) and ANS alone (○). The correlations time are 13.2 ns for apomyoglobin-ANS and 97 ps for ANS alone.

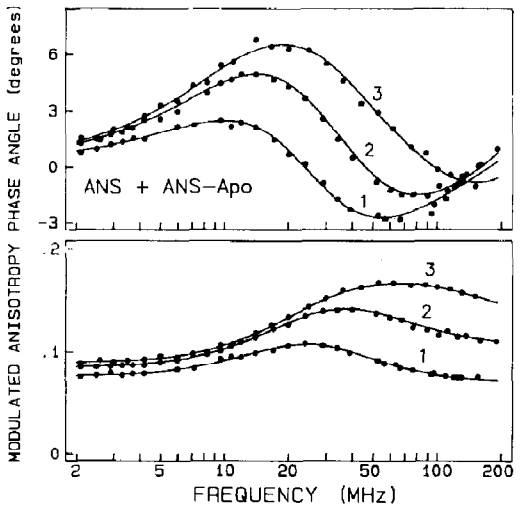

Fig. 7. Frequency-domain anisotropy data for apomyoglobin-ANS with molar ratios of 0.0087 (1), 0.0158 (2) and 0.079 (3).

individual analyses to 8.5 for the global analysis. It should be noted that the global analysis required the use of the intensity decay at each apomyoglobin/ANS ratio. The elevated value of χ^2_R probably represents the accumulated errors of these many experiments. The fact that the data from all these samples can be explained using these four parameters strongly suggests the two-species model is appropriate.

We also analyzed the data using the known values of r_0, and the decay times which are appropriate for the free and bound forms of ANS (0.255 and 15.67 ns). In this case, the analysis reveals the correlation times and the fractional intensity contributed by each form of ANS to the total emission. These values were found to be in agreement with the fractional intensities recovered from analysis of the individual intensity decays or from global analysis of all the intensity decays (table 3).

Table 3

Fractional intensities of ANS and ANS-apomyoglobin recovered from global analysis

The decay times were 255 ps and 15.67 ns, which were recovered from global analysis of the intensity decay data for 12 ANS/apomyoglobin ratios.

[Apo]/[ANS]	Single sample intensity decay	Global intensity decay	Global anisotropy decay
0	0.991	0.992	0.915
	0.009	0.008	0.085
0.0012	0.743	0.744	0.762
	0.257	0.256	0.238
0.0032	0.569	0.570	0.573
	0.431	0.430	0.427
0.0087	0.316	0.313	0.304
	0.684	0.687	0.696
0.0158	0.176	0.176	0.212
	0.824	0.824	0.788
0.0474	0.090	0.087	0.081
	0.910	0.913	0.919
0.0790	0.052	0.051	0.058
	0.948	0.949	0.942
1.183	0.040	0.006	0.005
	0.960	0.994	0.995

5. Discussion

The ANS-apomyoglobin system described here is clearly an extreme case which was selected to illustrate differences between associated and non-associated anisotropy decays. We suspect that in many cases it will be difficult to distinguish the associated and nonassociated models. Nonetheless, one can imagine a variety of macromolecular systems in which the associated model could be valuable. These systems include single-tryptophan proteins in two or more conformational states, proteins which contain two or more tryptophan residues, analysis of stepwise vs. continuous denaturation of proteins and fluorophores which partition between water and membranes or between distinct phases in a membrane, or of labelled proteins in cells which may be present in multiple environments. Additionally, the associated model can also be useful in analysis of data from samples in which some degree of fluorescent contamination is unavoidable, such as the weak tryptophan fluorescence from hemoglobin [25,26].

Acknowledgements

This work was supported by grants DMB-8511065 and DMB-0850285 from the National Science Foundation and GM-35154 from the National Institutes of Health. H.S. was on leave from the Pedagogical University, Institute of Physics, Slupsk, Poland, with partial support from CPBP 01.06.2.04 (Poland).

References

1 G. Weber, Biochem. J. 51 (1952) 145.
2 R.F. Steiner, Excited states of biopolymers, (Plenum Press, New York, 1983) p. 117.
3 G.G. Belford, R.L. Belford and G. Weber, Proc. Natl. Acad. Sci. U.S.A. 69 (1972) 1392.
4 E. Small and I. Isenberg, Biopolymers 16 (1977) 1907.
5 J.R. Lakowicz, Principles of fluorescence spectroscopy (Plenum Press, New York, 1983).
6 D.M. Rayner and A.G. Szabo, J. Am. Chem. Soc. 102 (1978) 554.
7 W.R. Laws, J.B.A. Ross, H.R. Wyssbrod, J. Beechem. L. Brand and J.C. Sutherland, Biochemistry 25 (1986) 599.

8 J.R. Lakowicz and H. Cherek, J. Biol. Chem. 255 (1980) 831.
9 J.R. Laws and L. Brand, J. Phys. Chem. 83 (1979) 795.
10 T.L. Nemzek and W.R. Ware, J. Chem. Phys. 62 (1975) 477.
11 J.R. Lakowicz, M.L. Johnson, N. Joshi, I. Gryczynski and G. Laczko, Chem. Phys. Lett. 131 (1986) 343.
12 J.R. Knutson, L. Davenport and L. Brand, Biochemistry 25, (1986) 1805.
13 L. Davenport, J.R. Knutson and L. Brand, Biochemistry 25 (1986) 1811.
14 J.R. Knutson, D.G. Walbridge and L. Brand, Biochemistry 21 (1982) 4671.
15 L.S. Stryer, J. Mol. Biol. 13 (1965) 482.
16 A. Jablonski, Bull. Acad. Pol. Sci. 8 (1960) 259.
17 R.D. Ludescher, L. Peting, S. Hudson and B. Hudson, Biophys. J. (1987) submitted for publication.
18 J.R. Lakowicz, H. Cherek, B. Maliwal and E. Gratton, Biochemistry 24 (1985) 376.
19 B.P. Maliwal and J.R. Lakowicz, Biochim. Biophys. Acta 873 (1986) 161.
20 F.W.J. Teale, Biochim. Biophys. Acta 35 (1959) 543.
21 J.R. Lakowicz and H. Cherek, Biochem. Biophys. Res. Commun. 99 (1981) 1173.
22 J.R. Lakowicz and B.P. Maliwal, Biophys. Chem. 21 (1985) 61.
23 J.R. Lakowicz, E. Gratton, H. Cherek and M. Linkemann, Biophys. J. 46 (1984) 463.
24 J.R. Lakowicz, G. Laczko and I. Gryczynski, Rev. Sci. Instrum. 57 (1986) 2499.
25 B. Alpert, D.M. Jameson and G. Weber, Photochem. Photobiol. 31 (1980) 1.
26 E. Bucci, H. Malak, C. Fronticelli, I. Gryczynski and J.R. Lakowicz, Proceedings of the G. Weber Symposium, Italy, 1987, in the press.